Wavelength and frequency doubling in impurity superlattices

Ahmet Elçi and David Depatie
Phillips Laboratory-LIDA, Kirtland Air Force Base, Albuquerque, New Mexico 87117
(Received 28 February 1992)

We discuss a special geometry of impurity superlattices that may produce wavelength and frequency doubling through a second-order nonlinear wave mixing. According to the band theory of impurity superlattices, the corresponding nonlinear susceptibility may become comparable to those found in ordinary crystals.

I. INTRODUCTION

The present crystal growth techniques can control impurity distributions in individual atomic layers.[1] With these techniques, it is possible to grow superlattices that have nearly wavelike impurity distributions. Figure 1 illustrates the wavelike donor and acceptor distributions, $p_D(\mathbf{r})$ and $p_A(\mathbf{r})$, respectively, given by

$$p_D(\mathbf{r})=N_0(1-\cos\mathbf{q}_0\cdot\mathbf{r}) ,$$
$$p_A(\mathbf{r})=N_0(1+\cos\mathbf{q}_0\cdot\mathbf{r}) . \tag{1}$$

Here, N_0 is half the amplitude of the impurity-density modulation. It is equal to the spatial averages of the donor and acceptor densities. $p_D(\mathbf{r})/(2N_0)$ $[p_A(\mathbf{r})/(2N_0)]$ is the probability of finding a donor [acceptor] impurity at position $\mathbf{r}$. $\mathbf{q}_0$ is along the superlattice axis. Its magnitude is given by $q_0=2\pi/\Lambda_0$, where Λ_0 is the superlattice period. The band theory of such superlattices[2] indicates that either the wavelength or the frequency of a coherent light beam may be doubled if an appropriate Λ_0 is chosen for a given pump frequency ω_p, and that this nonlinear wave mixing involves a second-order susceptibility. If performed, such nonlinear wave-mixing experiments may clarify the band theory of impurity superlattices. They may also lead to practically useful devices for frequency down and up conversion. In this paper we derive the relevant nonlinear susceptibility using the Brillouin-zone (BZ) folding theory of Ref. 2 for the impurity distribution.[1] This calculation shows that the nonlinear susceptibility is second order. For appropriate superlattice parameters, its magnitude may become comparable to the magnitude of the nonlinear susceptibility for homogeneous crystals that are used in two-wave mixing devices.

The theory of Ref. 2 takes into account the atomic nature of impurity charges. In this theory superlattice subbands arise from the broken symmetry of the original pure crystal. To the lowest order, it obtains energy-dispersion curves of subbands from the folding of the original BZ according to the superlattice period. The BZ folding, in conjunction with the screened impurity potential, also yields a hierarchy of selection rules for photon-induced transitions between conduction and valence subbands. In contrast, the only other theory of impurity superlattices[3] is based on a continuous jellium model (CJM) of impurity charges that does not yield any simple method for obtaining superlattice subband structures. Furthermore, in the CJM theory, photon-induced transitions are described by means of harmonic approximations and overlaps of harmonic oscillator wave functions[4] that do not yield any rigorous or approximate selection rules. The calculations of the present paper are exclusively based on the BZ folding theory of Ref. 2. Experimental verification of the theoretical results presented here would, therefore, be verification of the BZ folding theory.

Let us assume that we have a cubic crystal with the lattice constant a. Λ_0 and a are related by

$$\Lambda_0=La , \tag{2}$$

where L is an integer. The theory of Ref. 2 shows that each band of the pure crystal produces L superlattice subbands when it is doped according to the donor and acceptor distributions in (1). If L is an odd integer, then the superlattice subbands of a band n may be labeled by an index l that assumes the integer values in the interval

$$-\frac{(L-1)}{2}\le l\le\frac{(L-1)}{2} . \tag{3}$$

If L is an even integer, the labeling of subbands is slightly

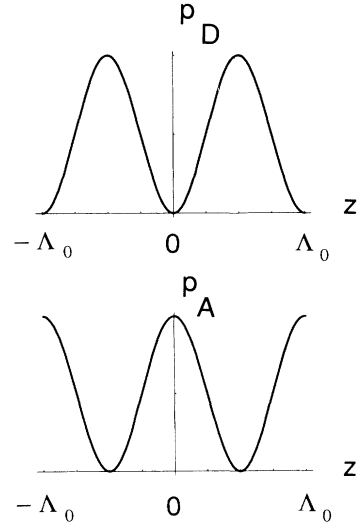

FIG. 1. Wavelike impurity distribution with period Λ_0.

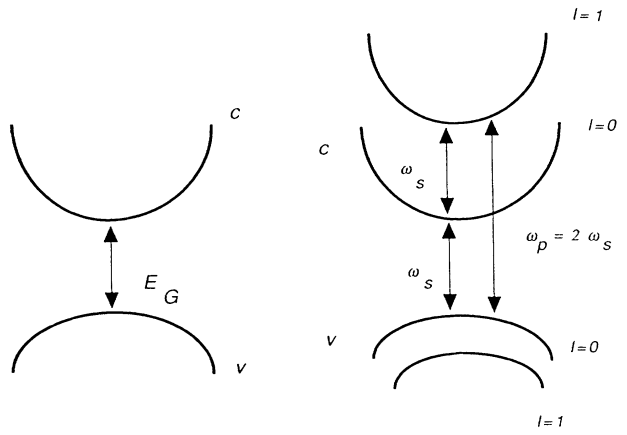

FIG. 2. Subband formation and wavelength doubling in an impurity superlattice.

more complicated and is given in Ref. 2. We assume that L is odd in the rest of the discussion. Let the wave vector $\mathbf{k}$ span the BZ of the pure crystal. In the superlattice geometry, this zone is partitioned into L subzones. The subzone centered on Γ becomes the superlattice BZ. The superlattice BZ is spanned by a wave vector κ given by

$$\kappa=\mathbf{k}-l\mathbf{q}_0 \ . \tag{4}$$

The superlattice subband energies are given by

$$E_{nl}(\kappa)=E_n^0(\kappa+l\mathbf{q}_0)+\delta E_{nl}(\kappa) \ , \tag{5}$$

where $E_n^0(\mathbf{k})$ is the band energy of the pure crystal and $\delta E_{nl}(\kappa)$ is a small correction term arising from the impurity potential. Equation (5) shows that the separation of subbands may be adjusted to a desired value by varying the superlattice period Λ_0. Let us consider the band structure illustrated in Fig. 2. Assume that the conduction and valence bands are parabolic near the center of the BZ, with the band energies

$$E_c^0(\mathbf{k})=E_G+\frac{\hbar^2\mathbf{k}^2}{2m_c} \ ; \quad E_v^0(\mathbf{k})=-\frac{\hbar^2\mathbf{k}^2}{2m_v} \ , \tag{6}$$

where E_G is the band gap, and m_c and m_v are the effective masses. In the figure we assumed that $m_c<m_v$. This assumption is made for the algebraic convenience of excluding the valence subband $l=1$ from the nonlinear wave-mixing process. If the crystal is doped according to the distributions in (1), then these bands are split into subbands whose states are labeled by $|cl\kappa\rangle$ and $|vl\kappa\rangle$. The figure shows only two subbands, $l=0$ and $l=1$, for c and v. Other subbands, such as those corresponding to $l=-1$ and $|l|>1$, are not shown in order not to clutter the figure. According to (5) and (6), the separation of the conduction subbands at $\kappa=0$ is approximately given by

$$E_{n1}(0)-E_{n0}(0)\simeq\frac{\hbar^2q_0^2}{2m_c}=\frac{2\pi^2\hbar^2}{m_c\Lambda_0^2} \ . \tag{7}$$

Therefore, if one adjusts the superlattice period to the value

$$\Lambda_0=\left[\frac{2\pi^2\hbar^2}{m_cE_G}\right]^{1/2} , \tag{8}$$

then the states $|v0,\kappa=0\rangle$, $|c0,\kappa=0\rangle$, and $|c1,\kappa=0\rangle$ compose a three-level system such that the energy separation of $|c1,\kappa=0\rangle$ and $|c0,\kappa=0\rangle$ equals the energy separation of $|c0,\kappa=0\rangle$ and $|v0,\kappa=0\rangle$, which is E_G. If κ is sufficiently small, the same is true for the states $|v0,\kappa\rangle$, $|c0,\kappa\rangle$, and $|c1,\kappa\rangle$. Clearly, if the optical-transition matrix elements between the pairs of the states $|v0,\kappa\rangle$ and $|c0,\kappa\rangle$, $|c0,\kappa\rangle$ and $|c1,\kappa\rangle$, and $|v0,\kappa\rangle$ and $|c1,\kappa\rangle$ are finite, then one can use this three-level system for either wavelength doubling or frequency doubling. The theory of Ref. 2 shows that these matrix elements are indeed finite. The optical coupling between $|v0,\kappa\rangle$ and $|c0,\kappa\rangle$ is the strongest; it is determined by the interband coupling of the original pure crystal. The couplings between the pairs $|c0,\kappa\rangle$ and $|c1,\kappa\rangle$, and $|v0,\kappa\rangle$ and $|c1,\kappa\rangle$ are weaker, since they are related to light absorption or emission by an electron in an impurity potential. Note that if $E_G=0.1$ eV, $m_c=0.1$ m, where m is the bare electron mass, then $\Lambda_0\approx 78$ Å, which is a reasonable value for the growing of a superlattice with the wavelike distribution, since impurity distributions are controlled in individual atomic layers whose widths are in the range 2–5 Å.

In Sec. II, we derive the nonlinear susceptibility for the wavelength doubling from the subband geometry shown in Fig. 2 and show that it is a second-order quantity. For $N_0\sim 10^{18}$ cm^{-3}, its value may be quite large, comparable to $\chi^{(2)}$ observed in homogeneous crystals of GaAs, InSb, InAs, and GaSb. In contrast to this result of the BZ folding theory, the CJM theory predicts a value which is at least 16 orders of magnitude smaller. In Sec. III, we derive the nonlinear susceptibility for the second-harmonic generation from the subband structure of Fig. 2. In the concluding section we briefly discuss other geometries and possible experimental observation.

II. WAVELENGTH DOUBLING

Let us assume that a pump wave of frequency $\omega_p\sim 2E_G$ is applied on the sample and a signal wave of frequency $\omega_s=\omega_p/2\sim E_G$ is generated. In the rotating-wave approximation, the electron-photon coupling Hamiltonian for the superlattice may be written as

$$H_{e\text{-}\gamma}=\sum_{\kappa}\{g_{cv}^s(\kappa)C_{c0\kappa}^\dagger C_{v0\kappa}a_s+g_{cv}^{s*}(\kappa)C_{v0\kappa}^\dagger C_{c0\kappa}a_s^\dagger+G_{cc}^s(\kappa)C_{c1\kappa}^\dagger C_{c0\kappa}a_s+G_{cc}^{s*}(\kappa)C_{c0\kappa}^\dagger C_{c1\kappa}a_s^\dagger$$
$$+G_{cv}^p(\kappa)C_{c1\kappa}^\dagger C_{v0\kappa}a_p+G_{cv}^{p*}(\kappa)C_{v0\kappa}^\dagger C_{c1\kappa}a_p^\dagger\} \ . \tag{9}$$

Here a_s ($a_s^\dagger$) and a_p ($a_p^\dagger$) are the annihilation (creation) operators for the signal and pump-wave photons. $C_{nl\kappa}$ ($C_{nl\kappa}^\dagger$) is the electron annihilation (creation) operator. The coupling coefficients $g_{nn'}^\mu$ and $G_{nn'}^\mu$ are given by[2]

$$g_{nn'}^\mu(\kappa)=\frac{eA_\mu}{mc}\epsilon_\mu\cdot\mathbf{p}_{nn'}(\kappa)\ , \tag{10}$$

$$G_{nn'}^\mu(\kappa)=W_0\sum_{n''}\left[\frac{\Phi_{nn''}(\kappa)g_{n''n'}^\mu(\kappa)}{E_n^0(\kappa+\mathbf{q}_0)-E_{n''}^0(\kappa)}+\frac{g_{nn''}^\mu(\kappa+\mathbf{q}_0)\Phi_{n''n'}(\kappa)}{E_{n'}^0(\kappa)-E_{n''}(\kappa+\mathbf{q}_0)}\right]\ . \tag{11}$$

Here, ϵ_μ is the polarization vector for the mode μ. A_μ is a constant given by

$$A_\mu=\left[\frac{2\pi\hbar^2c^2}{V_{\rm ol}n_\mu^2\omega_\mu}\right]^{1/2}\ , \tag{12}$$

where n_μ is the index of refraction and $V_{\rm ol}$ is the quantization volume. $\mathbf{p}_{nn'}$ is the matrix element of the momentum operator given by

$$\mathbf{p}_{nn'}(\kappa)=\delta_{nn'}\hbar\kappa+\mathbf{P}_{nn'}(\kappa)\ ,$$
$$\mathbf{P}_{nn'}(\kappa)=\sum_G\hbar\mathbf{G}\phi_n^*(\kappa+\mathbf{G})\Phi_{n'}(\kappa+\mathbf{G})\ , \tag{13}$$

where ϕ_n are the momentum Bloch functions[5] and $\mathbf{G}$ are the reciprocal-lattice vectors. W_0 is a constant related to the average density N_0:

$$W_0=\frac{4\pi N_0e^2}{\epsilon_0(q_0^2+q_s^2)}\ , \tag{14}$$

where ϵ_0 is the static dielectric constant and q_s is the screening wave vector (that is, q_s^{-1} is the screening length) for charged carriers. $\Phi_{nn'}(\kappa)$ represents an overlap of two momentum Bloch functions:

$$\Phi_{nn'}(\kappa)=\sum_G\phi_n^*(\kappa+\mathbf{q}_0+\mathbf{G})\phi_{n'}(\kappa+\mathbf{G})\ . \tag{15}$$

In order to calculate the nonlinear susceptibility for the wavelength doubling from the superlattice subbands of Fig. 2, we need to calculate the relevant second-order current density at time t, hence the second-order density matrix at time t.[6] We transform $H_{e\text{-}\gamma}$ to the interaction representation and split $H_{e\text{-}\gamma}(t)$ into two parts:

$$H_{e\text{-}\gamma}(t)=V_s(t)+V_p(t)\ , \tag{16}$$

where

$$V_s(t)=\sum_\kappa\{g_{cv}^s(\kappa)e^{i[E_{c0}(\kappa)-E_{v0}(\kappa)-\hbar\omega_s]t/\hbar}C_{c0\kappa}^\dagger C_{v0\kappa}a_s+G_{cc}^s(\kappa)e^{i[E_{c1}(\kappa)-E_{c0}(\kappa)-\hbar\omega_s]t/\hbar}C_{c1\kappa}^\dagger C_{c0\kappa}a_s+\text{H.c.}\}\ , \tag{17a}$$

$$V_p(t)=\sum_\kappa\{G_{cv}^p(\kappa)e^{i[E_{c1}(\kappa)-E_{v0}(\kappa)-\hbar\omega_p]t/\hbar}C_{c1\kappa}^\dagger C_{v0\kappa}+\text{H.c.}\}\ . \tag{17b}$$

The second-order density matrix in the interaction representation is given by

$$\rho_I^{(2)}(t)=-\frac{1}{\hbar^2}\int_{-\infty}^t dt'\int_{-\infty}^{t'}dt''[V_s(t')+V_p(t')\ ,\ [V_s(t'')+V_p(t''),\rho_0]]\ , \tag{18}$$

where ρ_0 is the initial density matrix at $t=-\infty$, given by

$$\rho_0=\rho_{\rm eq}\times\rho_F\ . \tag{19}$$

$\rho_{\rm eq}$ describes electrons in thermal equilibrium and ρ_F describes the electromagnetic field that has its two modes in coherent states. Therefore,

$$\text{Tr}[C_{nl\kappa}^\dagger C_{n'l'\kappa'}\rho_{\rm eq}]=\delta_{nn'}\delta_{ll'}\delta_{kk'}\frac{1}{[1+e^{\beta(E_{nl\kappa}-E_F)}]}\equiv\delta_{nn'}\delta_{ll'}\delta_{\kappa\kappa'}f(E_{nl\kappa})\ , \tag{20}$$

where $\beta=(k_BT)^{-1}$ is the inverse temperature and E_F is the Fermi energy. Similarly,

$$\frac{i}{c}\omega_\mu A_\mu\text{Tr}[a_\mu\rho_F]=E_\mu\quad\text{for }\mu=s\text{ or }p\ , \tag{21}$$

where E_s and E_p are the electric-field amplitudes of the signal and pump waves.

The terms that give rise to the wavelength doubling from the superlattice subbands of Fig. 2 come from the portion of the current-density operator which is proportional to $-(e/m)\mathbf{p}$ and is given by

$$\mathbf{J}_I^{\rm p}(t)=-\frac{e}{m}\sum_{nl\kappa;n'l'\kappa'}\mathbf{p}_{nl\kappa;n'l'\kappa'}\times e^{i[E_{nl}(\kappa)-E_{n'l'}(\kappa')]t/\hbar}C_{nl\kappa}^\dagger C_{n'l'\kappa'} \tag{22a}$$

in the interaction representation. Here,

$$\mathbf{p}_{nl\kappa;n'l'\kappa'}\simeq\delta_{\kappa\kappa'}\delta_{ll'}[\hbar(\kappa+l\mathbf{q}_0)\delta_{nn'}+\mathbf{P}_{nn'}(\kappa+l\mathbf{q}_0)]\ . \tag{22b}$$

Consider

$$\text{Tr}[C_{nl\kappa}^\dagger C_{n'l\kappa}\rho_I^{(2)}(t)]=-\frac{1}{\hbar^2}\int_{-\infty}^t dt'\int_{-\infty}^{t'}dt''\text{Tr}([[C_{nl\kappa}^\dagger C_{n'l\kappa}\ ,V_s(t')+V_p(t')]\ ,V_s(t'')+V_p(t'')]\rho_0)\ . \tag{23}$$

We rearranged the double commutator in the integrand for easier algebraic manipulation. The components of the current density oscillating at the signal frequency, that is, those proportional to $\exp[-i(\omega_p-\omega_s)t]=\exp[-i\omega_s t]$, come from the combination $V_s V_p$. Therefore, we need to evaluate only the portion of (23) given by

$$-\frac{1}{\hbar^2}\int_{-\infty}^{t}dt'\int_{-\infty}^{t'}dt''(\mathrm{Tr}\{[[[C^{\dagger}_{nl\kappa}C_{n'l\kappa},V_s(t')],V_p(t'')]\rho_0\}+\mathrm{Tr}\{[[[C^{\dagger}_{nl\kappa}C_{n'l\kappa},V_p(t')],V_s(t'')]\rho_0\}) . \tag{24}$$

Taking the indicated commutators, using (20) and (21), and picking those terms proportional to $\exp[-i(\omega_p-\omega_s)t]$, one finds

$$\begin{aligned}\{\mathrm{Tr}[C^{\dagger}_{nl\kappa}C_{n'l\kappa}\rho^{(2)}_I(t)]\}_{\text{relevant}}=&-\frac{n_s n_p V_{ol}}{2\pi\hbar^4\sqrt{\omega_s\omega_p}}\int_{-\infty}^{t}dt'\int_{-\infty}^{t'}dt''e^{-i[E_{c1}(\kappa)-E_{c0}(\kappa)-\hbar\omega_s]t'/\hbar}\\&\times e^{i[E_{c1}(\kappa)-E_{v0}(\kappa)-\hbar\omega_p]t''/\hbar}\\&\times\delta_{n,v}\delta_{n',c}\delta_{l,0}G^{s*}_{cc}(\kappa)G^{p}_{cv}(\kappa)\\&\times E_s^*E_p\{f[E_{v0}(\kappa)]-f(E_{c1}(\kappa)\}\ .\end{aligned} \tag{25}$$

Before we can proceed with the time integrals, we need to assign finite lifetimes to the states involved in the transitions in (25). Denote the linewidths associated with the transitions $|c1\kappa\rangle\leftrightarrow|v0\kappa\rangle$ and $|c1\kappa\rangle\leftrightarrow|c0\kappa\rangle$ by Γ and Γ':

$$\begin{aligned}\Gamma&=\frac{\hbar}{2}\left[\frac{1}{\tau_{c1\kappa}}+\frac{1}{\tau_{v0\kappa}}\right],\\ \Gamma'&=\frac{\hbar}{2}\left[\frac{1}{\tau_{c1\kappa}}+\frac{1}{\tau_{c0\kappa}}\right],\end{aligned} \tag{26}$$

where $\tau_{nl\kappa}$ is the lifetime of the state $|nl\kappa\rangle$. We now add appropriate imaginary parts to the band energies in order to take into account finite lifetimes of the states. This causes the exponential factors to vanish as $t\rightarrow-\infty$.[7] We make the replacements

$$\begin{aligned}E_{c1}(\kappa)&\rightarrow E_{c1}(\kappa)+i\frac{\hbar}{2\tau_{c1\kappa}}\ ,\\ E_{c0}(\kappa)&\rightarrow E_{c0}(\kappa)-i\frac{\hbar}{2\tau_{c0\kappa}}\ ,\end{aligned} \tag{27a}$$

in the first exponential and

$$\begin{aligned}E_{c1}(\kappa)&\rightarrow E_{c1}(\kappa)-i\frac{\hbar}{2\tau_{c1\kappa}}\ ,\\ E_{v0}(\kappa)&\rightarrow E_{v0}(\kappa)+i\frac{\hbar}{2\tau_{v0\kappa}}\ ,\end{aligned} \tag{27b}$$

in the second one. The exponential factors become

$$e^{-i[E_{c1}(\kappa)-E_{c0}(\kappa)-\hbar\omega_s+i\Gamma']t'/\hbar}e^{i[E_{c1}(\kappa)-E_{v0}(\kappa)-i\Gamma]t''/\hbar}\ . \tag{27c}$$

Finally, in order to determine the nonlinear susceptibility, we need to relate the current density to the polarization vector. This relation is given by

$$\langle\mathbf{J}\rangle(t)=\mathrm{Tr}[\mathbf{J}\rho(t)]=\mathrm{Tr}[\mathbf{J}_I(t)\rho_I(t)]=\frac{\partial\mathbf{P}}{\partial t}\ . \tag{28a}$$

When $\langle\mathbf{J}\rangle$ and $\mathbf{P}$ are transformed to the frequency space, one obtains

$$\langle\mathbf{J}\rangle(\omega)=-i\omega\mathbf{P}(\omega)\ . \tag{28b}$$

Substituting (27c) for the exponentials in (25), performing the indicated time integrations, using the result for the trace of $\mathbf{J}^p_I$ with $\rho^{(2)}_I$, one finds that the nonlinear polarization vector relevant to the down conversion $\omega_p\rightarrow\omega_s+\omega_s$ is given by

$$\begin{aligned}\mathbf{P}_{\omega_p\rightarrow\omega_s+\omega_s}(t)=&e^{-i(\omega_p-\omega_s)t}\frac{ie^3E_s^*E_p}{m^3\omega_s\omega_p(\omega_p-\omega_s)}\\&\times\sum_{\kappa}\mathbf{p}_{vc}(\kappa)\epsilon_s\cdot\mathbf{p}^{(\mathrm{SL})}_{cc}(\kappa)\epsilon_p\cdot\mathbf{p}^{(\mathrm{SL})}_{cv}(\kappa)\frac{\{f[E_{v0}(\kappa)]-f[E_{c1}(\kappa)]\}}{[E_{c1}(\kappa)-E_{v0}(\kappa)-\hbar\omega_p-i\Gamma][E_{c0}(\kappa)-E_{v0}(\kappa)+\hbar\omega_s-\hbar\omega_p-i(\Gamma+\Gamma')]}\ ,\end{aligned} \tag{29a}$$

where

$$\begin{aligned}\mathbf{p}^{(\mathrm{SL})}_{cc}(\kappa)&=W_0\sum_n\left[\frac{\mathbf{p}_{cn}(\kappa)\Phi^*_{cn}(\kappa)}{E^0_c(\kappa+\mathbf{q}_0)-E^0_n(\kappa)}+\frac{\Phi^*_{nc}(\kappa)\mathbf{p}_{nc}(\kappa+\mathbf{q}_0)}{E^0_c(\kappa)-E^0_n(\kappa+\mathbf{q}_0)}\right],\\ \mathbf{p}^{(\mathrm{SL})}_{cv}(\kappa)&=W_0\sum_{n'}\left[\frac{\Phi_{cn'}(\kappa)\mathbf{p}_{n'v}(\kappa)}{E^0_c(\kappa+\mathbf{q}_0)-E^0_{n'}(\kappa)}+\frac{\mathbf{p}_{cn'}(\kappa+\mathbf{q}_0)\Phi_{n'v}(\kappa)}{E^0_v(\kappa)-E^0_{n'}(\kappa+\mathbf{q}_0)}\right].\end{aligned} \tag{29b}$$

The nonlinear susceptibility corresponding to $\mathbf{P}$ in (29a) is then given by

$$\chi^{(\mathrm{SL}-2)}_{\mu\nu\lambda}(\omega_p-\omega_s)=\frac{ie^3}{m^3\omega_s\omega_p(\omega_p-\omega_s)V_{ol}}$$
$$\times\sum_{\kappa}p^{\mu}_{vc}(\kappa)p^{(\mathrm{SL})\nu}_{cc}(\kappa)p^{(\mathrm{SL})\lambda}_{cv}(\kappa)\frac{\{f[E_{v0}(\kappa)]-f[E_{c1}(\kappa)]\}}{[E_{c1}(\kappa)-E_{v0}(\kappa)-\hbar\omega_p-i\Gamma][E_{c0}(\kappa)-E_{v0}(\kappa)+\hbar\omega_s-\hbar\omega_p-i(\Gamma+\Gamma')]}\ . \tag{30}$$

Let us reconsider the transitions described by (30). They are analogous to the following transitions in a pure crystal. Consider the band structure in Fig. 3 and suppose that a valence-band electron absorbs a ω_p photon and goes to a high-momentum state in the conduction band. Next, suppose that the electron simultaneously emits an ω_s photon and a phonon of momentum $\mathbf{q}$ (or absorbs a phonon of momentum $-\mathbf{q}$) and goes to the bottom of the conduction band. This second stage is simply the inverse of the free-carrier absorption.[8] The electron at the bottom of the conduction band then emits a ω_s photon and goes to the top of the valence band. Finally, it emits (or absorbs) a phonon and goes back to the valence-band state from which it started. Normally such a set of transitions would not produce the down conversion of the pump wave, since the phonon-momentum $\mathbf{q}$ in the emission or absorption is not restricted to a well-defined value in thermal equilibrium. If, however, a well-defined sound wave of momentum $\mathbf{q}$ exists in the crystal, which means that the phonon field has a coherently excited mode, then the nonlinear wave mixing and the consequent wavelength doubling is possible. Indeed, such transitions constitute the Brillouin scattering of light.[9] It follows that the periodic distribution of impurities takes the place of a coherent excitation of the phonon field. The superlattice acts as a coherent source of momentum $\mathbf{q}_0$ and allows the nonlinear wave mixing to take place. The impurity superlattice has an advantage over the phonon field in that it is static and does not exchange energy with the electron during the wave-mixing process.

The homogeneous crystal band structure chosen in Fig. 2 assumes that the conduction and valence bands are well separated in energy from the other bands. Clearly, when the homogeneous crystal bands are folded onto the superlattice BZ and one obtains the illustrated subband structure, the conduction and valence subbands must still be well separated in energy from the subbands of the other bands. This means that the sums over the bands in $\mathbf{p}^{(\mathrm{SL})}_{cc}$ and $\mathbf{P}^{(\mathrm{SL})}_{cv}$ may be restricted to the conduction and valence bands alone. $\mathbf{p}^{(\mathrm{SL})}_{cc}$ becomes

$$\mathbf{p}^{(\mathrm{SL})}_{cc}(\kappa)\approx W_0\left[\frac{\mathbf{p}_{cv}(\kappa)\Phi^*_{cv}(\kappa)}{E^0_c(\kappa+\mathbf{q}_0)-E^0_v(\kappa)}+\frac{\mathbf{p}^*_{cv}(\kappa+\mathbf{q}_0)\Phi^*_{vc}(\kappa)}{E^0_c(\kappa)-E^0_v(\kappa+\mathbf{q}_0)}\right]. \tag{31}$$

If we expand the momentum Bloch function $\phi_n(\kappa+\mathbf{q}_0+\mathbf{G})$ around $\mathbf{q}_0=0$, we find[2,5]

$$\Phi^*_{nn'}(\kappa)=\delta_{nn'}-i\mathbf{q}_0\cdot\mathbf{X}_{nn'}(\kappa)+O(q_0^2)\ , \tag{32}$$

where $\mathbf{X}_{nn'}$ is the part of the position operator given by

$$\mathbf{X}_{nn'}(\mathbf{k})=i\sum_{\mathbf{G}}\phi^*_n(\mathbf{k}-\mathbf{G})\frac{\partial}{\partial\mathbf{k}}\phi_{n'}(\mathbf{k}-\mathbf{G})\ . \tag{33}$$

Note that $\mathbf{X}_{cv}$ and $\mathbf{P}_{cv}$ are related by

$$\mathbf{X}_{cv}(\mathbf{k})=\frac{-i\hbar\mathbf{P}_{cv}(\mathbf{k})}{m[E^0_c(\mathbf{k})-E^0_v(\mathbf{k})]}\ . \tag{34}$$

Using (32) and (34), as well as the approximations

$$E^0_c(\kappa+q_0)\approx E^0_c(\kappa)+E^0_G\ ,$$
$$E_c(\kappa)-E^0_v(\kappa+\mathbf{q}_0)\approx E_G\ ,\quad E^0_c(\kappa)-E^0_v(\kappa)\approx E_G\ , \tag{35}$$
$$\mathbf{P}_{cv}(\kappa+\mathbf{q}_0)\approx\mathbf{P}_{cv}(\kappa)\approx\mathbf{P}_{cv}(0)\ ,$$

we find

$$\mathbf{p}^{(\mathrm{SL})}_{cc}\approx-\frac{W_0}{2mE^2_G}[\hbar\mathbf{q}_0\cdot\mathbf{P}_{cv}]\mathbf{P}_{cv}\ . \tag{36}$$

Next, consider $\mathbf{p}^{(\mathrm{SL})}_{cv}$:

$$\mathbf{p}^{(\mathrm{SL})}_{cv}(\kappa)\simeq W_0\left\{\frac{\phi_{cc}(\kappa)\mathbf{p}_{cv}(\kappa)}{E^0_c(\kappa+\mathbf{q}_0)-E^0_c(\kappa)}+\frac{\mathbf{p}_{cv}(\kappa+\mathbf{q}_0)\Phi_{vv}(\kappa)}{E^0_V(\kappa)-E^0_v(\kappa+\mathbf{q}_0)}+\frac{\Phi_{cv}(\kappa)}{E^0_c(\kappa+\mathbf{q}_0)-E^0_v(\kappa)}\times[\mathbf{p}_{cc}(\kappa+\mathbf{q}_0)+\mathbf{p}_{vv}(\kappa)]\right\}. \tag{37}$$

Note that the energy denominator

$$[E^0_v(\kappa)-E^0_v(\kappa+\mathbf{q}_0)]$$

in (37) cannot be made smaller than W_0. The theory of

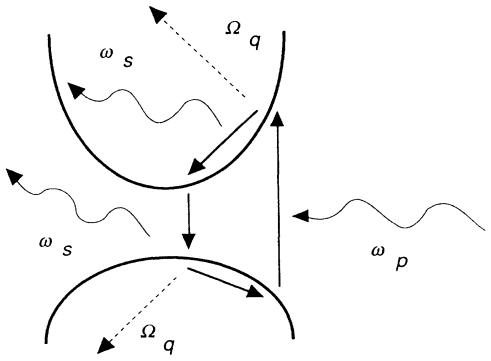

FIG. 3. A possible phonon-assisted frequency down conversion in a homogeneous crystal.

Ref. 2, in particular, Eq. (11), is derived under the assumption that the zeroth-order subband energies $E_n^0(\kappa+l\mathbf{q}_0)$ are not degenerate. Thus, one must have

$$W_0 < |E_v^0(\kappa+\mathbf{q}_0)-E_v^0(\kappa)| \ , \ |E_c^0(\kappa+\mathbf{q}_0)-E_c^0(\kappa)| \ . \quad (38)$$

If $|\mathbf{q}_0|$ is decreased (hence, Λ_0 is increased) to a value that violates (38), one may not use Eq. (11). Instead, one must calculate $G_{nn'}^{\mu}$ from a degenerate perturbation theory, along the lines suggested in Ref. (2). Actually we will assume that

$$|E_v^0(\kappa)-E_v^0(\kappa+\mathbf{q}_0)|$$

is of the same order of magnitude as E_G, even though $m_v > m_c$, and approximate the first two terms of (37) by $(2W_0/E_G)\mathbf{P}_{cv}$. Although this yields an underestimate of $\mathbf{p}_{cv}^{(\mathrm{SL})}$, it is sufficient for an order-of-magnitude calculation. We should add that the assumption of nondegeneracy puts a restriction on the use of the parabolic-band approximation, since this approximation may give rise to degeneracy as one approaches the boundaries of the superlattice BZ. Consider, for example, $E_c^0(\kappa+\mathbf{q}_0)$ and $E_c^0(\kappa)$. Set $\kappa=-\mathbf{q}_0/2$. $E_c^0(\mathbf{q}_0/2)$ and $E_c^0(-q_0/2)$ are degenerate in the parabolic-band approximation. In order to avoid such degeneracies, the parabolic-band approximation Eq. (6) must be restricted to the center of the superlattice BZ. We assume that actual zeroth-order subband energies are not parabolic and that $E_{c,v}^0(\mathbf{q}_0/2)$ differs from $E_{c,v}^0(-\mathbf{q}_0/2)$. In fact, we assume that

$$W_0 < \left| E_{c,v}^0\left[\frac{\mathbf{q}_0}{2}\right]-E_{c,v}^0\left[-\frac{q_0}{2}\right]\right| . \quad (39)$$

For the last group of terms in (37), we note that the intraband momentum matrix elements are given by[10]

$$\mathbf{p}_{cc}(\kappa+\mathbf{q}_0)\simeq\frac{\hbar(\kappa+\mathbf{q}_0)}{m_c} \ , \ \mathbf{p}_{vv}(\kappa)\simeq-\frac{\hbar\kappa}{m_v} \ . \quad (40)$$

Taking the leading terms for $\Phi_{nn'}$, we finally obtain

$$\begin{aligned}\mathbf{p}_{cv}^{(\mathrm{SL})}(\kappa)&\approx\frac{2W_0}{E_G}\mathbf{P}_{cv}+\frac{iW_0\mathbf{q}_0\cdot\mathbf{P}_{cv}}{2mE_G^2}\\&\quad\times\left[\hbar\kappa\left[\frac{1}{m_c}-\frac{1}{m_v}\right]+\frac{\hbar\mathbf{q}_0}{m_c}\right]\\&\approx\frac{2W_0}{E_G}\mathbf{P}_{cv} \ .\end{aligned} \quad (41)$$

Using (36) and (41), the nonlinear susceptibility becomes

$$\begin{aligned}\chi_{\mu\nu\lambda}^{(\mathrm{SL}\text{-}2)}(\omega_p-\omega_s)\approx&-\left[\frac{W_0}{E_G}\right]^2\frac{ie^3\hbar\mathbf{q}_0\cdot\mathbf{P}_{cv}}{m^4\omega_s\omega_p(\omega_p-\omega_s)E_GV_{ol}}P_{cv}^{*\mu}P_{cv}^{\nu}P_{cv}^{\lambda}\\&\times\sum_{\kappa}\frac{\{f[E_{v0}(\kappa)]-f[E_{c1}(\kappa)]\}}{[E_{c1}(\kappa)-E_{v0}(\kappa)-\hbar\omega_p-i\Gamma][E_{c0}(\kappa)-E_{v0}(\kappa)+\hbar\omega_s-\hbar\omega_p-i(\Gamma+\Gamma')]} \ .\end{aligned} \quad (42)$$

In order to get a feeling about the magnitude of $\chi^{(\mathrm{SL}\text{-}2)}$, let us assume that $E_G\sim0.1$ eV, $\epsilon_0\sim20$, $q_0\sim q_s\sim2\pi\times10^6$ cm^{-1}, and $N_0\sim10^{18}$ cm^{-3}. This yields $W_0\sim10^{-3}$ eV and $(W_0/E_G)\sim10^{-2}$. Let the linewidths Γ and Γ' be on the order of 10^{-2} eV. This corresponds to a lifetime of about 10^{-13} sec. Let us take $P_{cv}/\hbar\sim10^7$ cm^{-1}. Let us also approximate the energy denominators in (42) at their resonance values and pull them out of the integral. Neglecting the higher conduction subband occupation, the remaining integral over κ yields the total density of electrons in the highest valence subband:

$$N_{v0}=(v_{ol})^{-1}\sum_{\kappa}f[E_{v0}(\kappa)] \ .$$

N_{v0} is on the order of $(a^2\Lambda_0)^{-1}$, where a is the lattice constant of the pure crystal and Λ_0 is the superlattice period. For $a\sim5$ Å and $\Lambda_0\sim100$ Å, one has $N_{v0}\sim3\times10^{20}$ cm^{-3}. Thus, we find

$$\begin{aligned}|\chi^{(\mathrm{SL}\text{-}2)}|&\approx\frac{e^3W_0^2\hbar^4q_0N_{v0}P_{cv}^4}{4m^4E_G^4\Gamma^2}\\&\approx10^{-6}\text{ cgs units} \ .\end{aligned} \quad (43)$$

This value is on the order of $\chi^{(2)}$ for homogeneous crystals of GaAs, InSb, InAs, and GaSb.[11]

The order-of-magnitude estimate in (43) must be viewed as generic. In Sec. IV, we consider specific semiconductors in conjunction with proposed experiments. Because of degeneracy, or near degeneracy, the subband structure of common semiconductors may become considerably more complicated than the structure illustrated in Fig. 2.

It is important to note that the result in Eq. (43) is totally at variance with the CJM theory of Ref. 4. In that theory, spatially separated electrons and holes are assumed to feel nearly harmonic potentials. The matrix elements between the conduction and valence harmonic levels are reduced relative to the pure crystal by an exponential factor:

$$g_{cv}^{\mathrm{SL}}\sim|P_{cv}|\exp\left[-\frac{4W_0}{\hbar\omega_{\mathrm{pl}}}\right] , \quad (44)$$

where ω_{pl} is the plasma frequency of the free carriers. Döhler and Ruden estimate that for the relatively stronger transitions from the lowest conduction subband to the highest light-hole subband in III–V semiconductors, the exponential factor has the magnitude 10^{-7}. For the heavy-hole subbands, the same factor becomes 10^{-10}. Thus, the CJM predicts, on the basis of the reduction of the matrix element alone, a $\chi^{(\mathrm{SL}\text{-}2)}$ on the order of 10^{-23} cgs units or less.

III. FREQUENCY DOUBLING

We now assume that a pump wave of frequency $\omega_p \sim E_G$ is incident on the superlattice sample and a signal wave of frequency $\omega_s = 2\omega_p$ is generated. The transitions involved in this second harmonic generation are shown in Fig. 4. If we interchange s and p indices in Eq. (9), we obtain the interaction Hamiltonian for the frequency-doubling process in Fig. 3:

$$H_{e\text{-}\gamma} = \sum_{\kappa} \{ g^{p}_{cv}(\kappa) C^{\dagger}_{c0\kappa} C_{v0\kappa} a_p + g^{p*}_{cv}(\kappa) C^{*}_{v0\kappa} C_{c0\kappa} a^{\dagger}_p + G^{p}_{cc}(\kappa) C^{\dagger}_{c1\kappa} C_{c0\kappa} a_p + G^{p*}_{cc}(\kappa) C^{\dagger}_{c0\kappa} C_{c1\kappa} a^{\dagger}_p + G^{s}_{cv}(\kappa) C^{\dagger}_{c1\kappa} C_{v0\kappa} a_s + G^{s*}_{cv}(\kappa) C^{\dagger}_{v0\kappa} C_{c1\kappa} a^{\dagger}_s \} \ . \tag{45}$$

In order to calculate the nonlinear susceptibility, we need to calculate the component of the polarization oscillating as $\exp[-i(\omega_p+\omega_p)t] = \exp[-i\omega_s t]$. It is clear from Fig. 4 that the nonlinear current density yielding this component of the polarization arises from the matrix element of the superlattice momentum operator connecting the subbands $c1$ and $v0$. We infer from Eq. (11) that this matrix element is given by

$$\mathbf{p}^{(\mathrm{SL})}_{c1\kappa;v0\kappa} = W_0 \sum_{n} \left[\frac{\Phi_{cn}(\kappa)\mathbf{p}_{nv}(\kappa)}{E^0_c(\kappa+\mathbf{q}_0) - E^0_n(\kappa)} + \frac{\mathbf{p}_{cn}(\kappa+\mathbf{q}_0)\Phi_{nv}(\kappa)}{E^0_v(\kappa) - E^0_n(\kappa+\mathbf{q}_0)} \right] . \tag{46}$$

The corresponding current-density operator in the interaction representation is given by

$$\mathbf{J}^{\mathrm{SH}}_I(t) = -\frac{e}{m} \sum_{\kappa} \mathbf{p}^{(\mathrm{SL})*}_{c1\kappa;v0\kappa} e^{i[E_{v0}(\kappa) - E_{c1}(\kappa)]t/\hbar} C^{\dagger}_{v0\kappa} C_{c1\kappa} \ . \tag{47}$$

Using (18), we see that the second-harmonic current density is associated with the $\langle a_p a_p \rangle$ terms in the integral of the double commutator

$$\left\{ -\frac{1}{\hbar^2} \int_{-\infty}^{t} dt' \int_{-\infty}^{t'} dt'' \mathrm{Tr}([[C^{\dagger}_{v0\kappa} C_{c1\kappa}, V_p(t')], V_p(t'')]\rho_0) \right\}_{\mathrm{SH}}$$
$$= \frac{e^{-2i\omega_p t} e^{i[E_{c1}(\kappa) - E_{v0}(\kappa)]t/\hbar} g^{p}_{cv}(\kappa) G^{p}_{cc}(\kappa) \langle a_p a_p \rangle}{[E_{c1}(\kappa) - E_{v0}(\kappa) - 2\hbar\omega_p - i\Gamma_0 - i\Gamma']}$$
$$\times \left[\frac{f[E_{v0}(\kappa)] - f[E_{c0}(\kappa)]}{E_{c0}(\kappa) - E_{v0}(\kappa) - \hbar\omega_p - i\Gamma_0} + \frac{f[E_{c0}(\kappa)] - f[E_{c1}(\kappa)]}{E_{c1}(\kappa) - E_{c0}(\kappa) - \hbar\omega_p - i\Gamma'} \right] , \tag{48}$$

where Γ_0 is the linewidth associated with the transition $|c0\kappa\rangle \leftrightarrow |v0\kappa\rangle$. The polarization is given by

$$\mathbf{P}_{\omega_p+\omega_p\to\omega_s} = e^{-2i\omega_p t} \frac{ie^3 E_s E_s}{2m^3\omega_p^3} \sum_{\kappa} \mathbf{p}^{(\mathrm{SL})*}_{c1\kappa;v0\kappa} \boldsymbol{\epsilon}_p \cdot \mathbf{p}_{cv}(\kappa) \boldsymbol{\epsilon}_p \cdot \mathbf{p}^{(\mathrm{SL})}_{cc}(\kappa) \frac{1}{[E_{c1}(\kappa) - E_{v0}(\kappa) - 2\hbar\omega_p - i\Gamma_0 - i\Gamma']}$$
$$\times \left[\frac{f[E_{v0}(\kappa)] - f[E_{c0}(\kappa)]}{E_{c0}(\kappa) - E_{v0}(\kappa) - \hbar\omega_p - i\Gamma_0} + \frac{f[E_{c0}(\kappa)] - f[E_{c1}(\kappa)]}{E_{c1}(\kappa) - E_{c0}(\kappa) - \hbar\omega_p - i\Gamma'} \right] . \tag{49}$$

The nonlinear susceptibility for frequency doubling becomes

$$\chi^{(\mathrm{SL}\text{-}2)}_{\mu\nu\lambda}(\omega_p + \omega_p = \omega_s) = \frac{ie^3}{2m^3\omega_p^3 V_{ol}} \sum_{\kappa} p^{(\mathrm{SL})*\mu}_{c1\kappa;v0\kappa} p^{\nu}_{cv}(\kappa) p^{(\mathrm{SL})\lambda}_{cc}(\kappa) \frac{1}{[E_{c1}(\kappa) - E_{v0}(\kappa) - 2\hbar\omega_p - i\Gamma_0 - i\Gamma']}$$
$$\times \left[\frac{f[E_{v0}(\kappa)] - f[E_{c0}(\kappa)]}{E_{c0}(\kappa) - E_{v0}(\kappa) - \hbar\omega_p - i\Gamma_0} + \frac{f[E_{co}(\kappa)] - f[E_{c1}(\kappa)]}{E_{c1}(\kappa) - E_{c0}(\kappa) - \hbar\omega_p - i\Gamma'} \right] . \tag{50}$$

Comparing (50) with (30), one sees that

$$\chi^{(\mathrm{SL}\text{-}2)}(\omega_p + \omega_p = \omega_s)$$

is of the same order of magnitude as

$$\chi^{(\mathrm{SL}\text{-}2)}(\omega_p - \omega_s = \omega_s) \ .$$

Thus, the proposed impurity superlattice geometry would be an extremely efficient second-harmonic generator.

IV. CONCLUDING REMARKS

As far as the frequency tunability of the proposed two-wave mixing process is concerned, the geometry of Fig. 2 has a slight disadvantage in that it uses a transition across the band gap of the crystal for the mixing of two waves. This allows the nonlinear susceptibilities (30) and (50) to be quite large, but restricts either the pump frequency or the signal frequency to a small neighborhood around $E_G/\hbar$. If one is willing to tolerate smaller non-

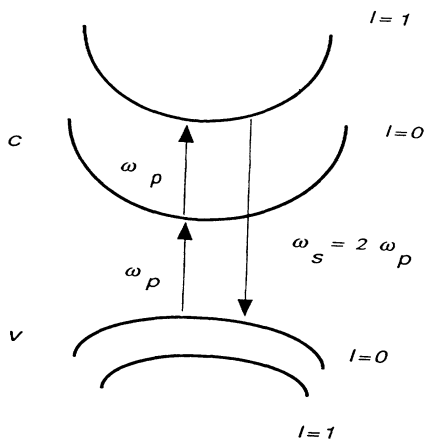

FIG. 4. Second-harmonic generation from the superlattice subbands.

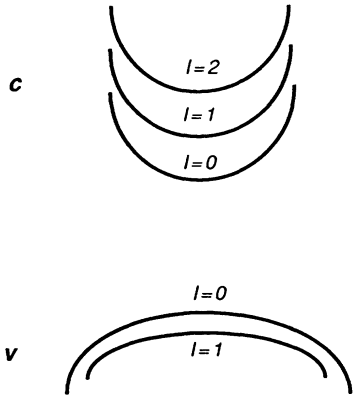

FIG. 5. A different subband structure for second-order wave mixing.

linear susceptibilities, one may achieve a greater frequency tunability with impurity superlattices. As an example, let us assume that the crystal is doped only with donors with a superlattice period $\Lambda_0 \sim 300$ Å. All other parameters for the pure crystal remaining the same as before, one has the subband structure illustrated in Fig. 5. One may therefore use $l=0$, 1, and 2 subbands of the conduction band for two-wave mixing. The matrix elements for the transitions

$$|c,l=0,\kappa\rangle \leftrightarrow |c,l=1,\kappa\rangle$$

and

$$|c,l=1,\kappa\rangle \leftrightarrow |c,l=2,\kappa\rangle$$

are essentially the same as before, given by G_{cc}^{μ} of Eq. (11). The theory of Ref. 2 indicates that the matrix element connecting the states $|c,l=2,\kappa\rangle$ and $|c,l=0,\kappa\rangle$ is on the order of $(W_0/E_G)G_{cc}^{\mu}$. Thus, the magnitude of a second-order nonlinear susceptibility using only the conduction subbands for two-wave mixing is reduced compared to (30) and (50) by a factor $(W_0/E_G)^2 \sim 10^{-4}$. Note that this would still yield a substantial second-order nonlinear susceptibility which is on the order of $10^{-2}\times\chi^{(2)}$ for potassium dihydrogen phosphate.

The preceding calculations indicate that the proposed two-wave mixing mechanism of Fig. 2 may be readily observable in impurity superlattices of III–V semiconductors, for example, in InSb. When doped according to (1), the actual subband structure of InSb would be much more complicated than the simple structure illustrated in Fig. 2. There are three sources of this complexity. The multiple folding of the BZ is one. As L becomes a larger integer, more subzones are created. The pieces of the original energy-dispersion curves of the conduction and valence bands that fall into the additional subzones produce more subbands. The spin-orbit coupling is the second source of the complexity. In InSb and in similar semiconductors, the spin-orbit coupling is significant and determines the main features of the band structure of pure crystals. The use of an appropriate Kane model for the original homogeneous bands in the preceding calculations may ameliorate the neglect of the spin-orbit coupling in the theory of Ref. 2 to some extent. Nevertheless, one should keep in mind that the spin-orbit coupling may affect selection rules as the original BZ is folded. The third source of the complexity is the near-spherical symmetry of the bands of InSb in the neighborhood of Γ. This symmetry leads to the crossing of the folded bands for $\pm|l|$ as illustrated on the left-hand side of Fig. 6 for $l=+1$ and $l=-1$. Without the coupling induced by the impurity potential, these two subbands cross each other. Within the circled region, the two subbands may be treated as degenerate. If the coupling induced by the impurity potential is taken into account, the two subband energies are approximately given by

$$E_{n\pm}(\kappa)=\tfrac{1}{2}[E_n^0(\kappa+q_0)+E_n^0(\kappa-q_0)]\pm\frac{1}{2}\sqrt{[E_n^0(\kappa+q_0)-E_n^0(\kappa-q_0)]^2+4|W_{n,1,\kappa;n,-1,\kappa}|^2}\ , \tag{51}$$

where $W_{nl\kappa;n'l'\kappa'}$ is the matrix element associated with the impurity potential and is given by[2]

$$W_{nl\kappa;n'l'\kappa'}=\delta_{\kappa\kappa'}W_0\sum_G\{\delta_{l,l'+1}\phi_n^*(\kappa+lq_0-G)\phi_{n'}[\kappa+(l-1)q_0-G] + \delta_{l+1,l'}\phi_n^*(\kappa+lq_0-G)\phi_{n'}[\kappa+(l+1)q_0-G]\}\ . \tag{52}$$

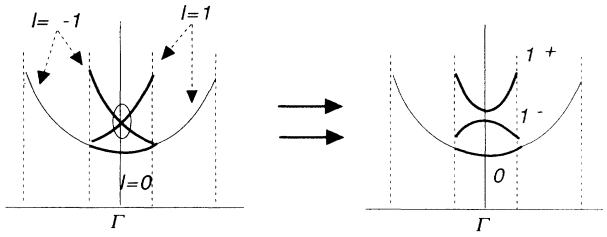

FIG. 6. The left-hand figure shows the pure BZ folding and the crossing of two subbands. The right-hand figure shows the subbands avoiding the crossing due to the impurity potential.

With the avoided crossing as illustrated on the right-hand side of Fig. 6, a subband is no longer exclusively related to just one of the subzones of the original BZ. For example, the two pieces of the highest subband in the right figure of Fig. 6, beginning from Γ and extending in the directions $+\hat{\kappa}$ and $-\hat{\kappa}$, are mostly the contributions of the subzones spanned by $\kappa-q_0$ and $\kappa+q_0$, respectively.

We should add that these complications do not affect the order-of-magnitude estimates obtained in the preceding sections. They simply require some fine tuning of theoretical calculations for specific semiconductors. Indeed, in some cases they may actually increase the magnitude of $\chi^{(SL-2)}$ by multiplying (30) and (50) with appropriate degeneracy factors.

ACKNOWLEDGMENTS

We thank A. Ongstad, N. Pchelkin, and P. Sharma for many useful discussions.

[1]E. F. Schubert, J. E. Cunningham, and W. T. Tsang, Phys. Rev. B **36**, 1348 (1987).
[2]A. Elçi, Phys. Rev. B **45**, 2208 (1992).
[3]P. Ruden and G. H. Döhler, Phys. Rev. B **27**, 3538 (1983); **27**, 3547 (1983).
[4]G. H. Döhler and P. Ruden, Phys. Rev. B **30**, 5932 (1984).
[5]A. Elçi and E. D. Jones, Phys. Rev. B **34**, 8611 (1986).
[6]C. Flytzanis, edited by H. Rabin and C. L. Tang (Academic, New York, 1975), Vol. I, Pt. A.
[7]This is equivalent to the method that assumes that the band energies have imaginary parts to begin with and constructs a non-Hermitian matrix from these. This matrix anticommutes with the density matrix in the equation of motion.
[8]A. Elçi, M. O. Scully, A. L. Smirl, and J. C. Matter, Phys. Rev. B **16**, 191 (1977).
[9]A. Yariv, *Quantum Electronics* (Wiley, New York, 1975), Chap. 18.
[10]H. J. Meyer, Phys. Rev. **112**, 298 (1958).
[11]N. Bloembergen, *Nonlinear Optics* (Benjamin, New York, 1965), Chap. 5.